Biological Sciences: Environmental Sciences

The genome sequence of the Button Mushroom *Agaricus bisporus* reveals mechanisms governing adaptation to a humic-rich ecological niche

E Morin[a,2], A Kohler[a,2], A Baker[b,2], M Foulongne-Oriol[c,2], V Lombard[d], LG Nagy[e], RA Ohm[f,g], A Patyshakuliyeva[h], A Brun[a], AL Aerts[f], AM Bailey[i], C Billette[c], PM Coutinho[d], G Deakin[j], H Doddapaneni[k], D Floudas[e], J Grimwood[l], K Hildén[m], U Kües[n], KM LaButti[f], A Lapidus[f], EA Lindquist[f], SM Lucas[f], T Lundell[m], C Murat[a], RW Riley[f], AA Salamov[f], J Schmutz[g], V Subramanian[o], HAB Wösten[g], JP Xu[p], DC Eastwood[q], GD Foster[i], ASM Sonnenberg[r], D Cullen[s], R P. de Vries[h], DS Hibbett[e], B Henrissat[d], KS Burton[j], RW Kerrigan[t], MP Challen[u,2], IV Grigoriev[f,1,2] & F Martin[a,1,2]

[a] *INRA, UMR1136 INRA/UHP, Interactions Arbres/ Micro-organismes, Centre de Nancy, 54280 Champenoux, France.*
[b] *University of Warwick, Wellesbourne, Warwick CV35 9EF, UK.*
[c] *INRA, UR1264 MYCSA, F-33883 Villenave d'Ornon, France.*
[d] *Aix-Marseille Université, CNRS UMR 7257, 13288 Marseille Cedex 9, France.*
[e] *Biology Department, Clark University, Worcester, MA 01610, USA.*
[f] *U.S. Department of Energy Joint Genome Institute, Walnut Creek, CA 94598, USA.*
[g] *Microbiology, Utrecht University, Padualaan 8, 3584 CH Utrecht, Netherlands.*
[h] *CBS-KNAW Fungal Biodiversity Centre, Uppsalalaan 8, 3584 CT Utrecht, Netherlands.*
[i] *School of Biological Sciences, University of Bristol, Woodland Rd, Bristol, BS8 1UG, U.K.*
[j] *East Malling Research, New Road, East Malling, Kent, ME19 6BJ, UK*
[k] *Carver Center for Genomics, Department of Biology, University of Iowa, Iowa City, IA, 52242, USA*
[l] *U.S. Department of Energy Joint Genome Institute, Hudson Alpha Institute.*
[m] *University of Helsinki, Division of Microbiology, Viikki Biocenter 1, Department of Food and Environmental Sciences, FI-00014, Finland.*
[n] *Molecular Wood Biotechnology and Technical Mycology, Bu□sgen-Institute, Georg-August-University, D-37077 Göttingen, Germany*
[o] *Biosciences Center, National Renewable Energy Laboratory, Golden, CO, 80401, USA.*
[p] *Department of Biology, McMaster University, Hamilton, Ontario, L8S 4K1, Canada.*
[q] *College of Science, University of Swansea, Singleton Park, Swansea SA2 8PP, UK.*
[r] *Wageningen University, Plant Research International - Mushrooms P.O.Box 16, 6700 AA Wageningen.*
[s] *Forest Products Laboratory, Madison, WI 53726, USA.*
[t] *Sylvan Biosciences, 198 Nolte Dr., Kittanning, PA 16201, USA.*
[u] *Wellcome Trust Centre for Human Genetics, University of Oxford, Roosevelt Drive, Oxford, OX3 7BN, UK*

Abstract

Agaricus bisporus is the model fungus for the adaptation, persistence and growth in the humic-rich leaf litter environment. Aside from its ecological role, *A. bisporus* has been an important component of the human diet for over 200 years and worldwide cultivation of the 'button mushroom' forms a multi-billion dollar industry. We present two *A. bisporus* genomes, their gene repertoires and transcript profiles on compost and during mushroom formation. The genomes encode a full repertoire of polysaccharide-degrading enzymes similar to that of wood-decayers. Comparative transcriptomics of mycelium grown on defined medium, casing-soil and compost revealed genes encoding enzymes involved in xylan, cellulose, pectin and protein degradation are more highly expressed in compost. The striking expansion of heme-thiolate peroxidases and beta-etherases is distinctive from Agaricomycotina wood-decayers and suggests a broad attack on decaying lignin and related metabolites found in humic acid-rich environment. Similarly, up-regulation of these genes together with a lignolytic manganese peroxidase, multiple copper radical oxidases and cytochrome P450s is consistent with challenges posed by complex humic-rich substrates. The gene repertoire and expression of hydrolytic enzymes in *A. bisporus* is substantially different from the taxonomically-related ectomycorrhizal symbiont *Laccaria bicolor*. A common promoter motif was also identified in genes very highly expressed in humic-rich substrates. These observations reveal genetic and enzymatic mechanisms governing adaptation to the humic-rich ecological niche formed during plant degradation, further defining the critical role such fungi contribute to soil structure and carbon sequestration in terrestrial ecosystems. Genome sequence will expedite mushroom breeding for improved agronomic characteristics.

Keywords: Agaricomycotina, humic substances, litter decay, wood decay fungi, carbohydrate-active enzymes, humic-response element.

Author contributions: K.S.B., M.P.C., R.P.d.V., I.V.G., D.S.H., R.W.K. and F.M. designed research; E.M., A.K., A.B., M.F.O., V.L., R.A.O., A.P., A.B., A.L.A., A.M.B., C.B., P.M.C., G.D., H.D., D.F., J.G., D.S.H., K.H., U.K., K.M.L., A.L., E.A.L., S.M.L., T.L., C.M., L.G.N., R.W.R., A.A.S., J.S., V.S., H.A.B.W., J.P.X., D.C.E., G.D.F., A.S.M.S., D.C., R.P.d.V., B.H., K.S.B., R.W.K., M.P.C., I.V.G. and F.M. performed research and analyzed data; F.M., R.W.K., M.P.C. and K.S.B. wrote the paper with help from E.M., A.K., A.M.B., M.F.O., H.D., U.K., T.L., C.M., L.G.N., R.A.O., H.A.B.W., J.P.X., D.C.E., G.D.F., A.S.M.S., D.C., R.P.d.V., D.S.H., B.H. and I.V.G.

The authors declare no conflict of interest.

This article is a PNAS Direct Submission.

Data deposition: The sequences reported in this paper have been deposited in the GenBank database [accession nos. AEOK00000000 (*A. bisporus* H97) and AEOL00000000 (*A. bisporus* var. *burnettii*)]; the data reported in this paper have been deposited in the Gene Expression Omnibus (GEO) database, www.ncbi.nlm.nih.gov/geo [accession nos. 000)].

[1] To whom correspondence may be addressed. E-mail: *fmartin@nancy.inra.fr* and *ivgrigoriev@lbl.gov*.
[2] E.M., A.K., A.B. and MFO contributed equally to this work as first author. MPC, IG and FM contributed equally to this work as senior author

This article contains supporting information online at www.pnas.org/lookup/suppl/xxx.

\body

Introduction

The plant polymer complex lignocellulose is the most abundant organic compound in the terrestrial environment consisting of three main components: cellulose, hemicellulose and lignin (1). These polymers are decayed primarily by wood and litter decomposers from the Agaricomycotina (mushroom-forming fungi). Comparative analyses of the 'white-rot' fungi *Phanerochaete chrysosporium* and *Schizophyllum commune* (2, 3), the 'brown-rots' *Postia placenta* and *Serpula lacrymans* (4, 5), and the coprophilous *Coprinopsis cinerea* (6) has provided considerable insight into the evolution of the wood decomposition machinery in fungi. Much less is known about fungal decomposition of partially-degraded plant material, particularly leaf litter, and about adaptation to humic-rich environments. Improving knowledge of processes governing this adaptation is critical to improving carbon management and predictive modeling of terrestrial carbon cycling.

The biomass of non-woody litter in temperate woodlands can be 4–5 times greater than that of woody litter (7); equivalent to 1–2 gigatons of sequestered carbon per year or 15–30% of annual global emissions of carbon from fossil fuels and industrial activities. Concentrations of lignin and (hemi)cellulose in leaf litters of hardwood species range from 33-43% and 23-29%, respectively (8). After a succession of microbial colonisations the litter is substantially modified by the removal of readily available carbon, nitrogen and minerals, and the formation of humic substances. Humic substances originate from the decay of modified lignin and other recalcitrant aromatic compounds, and microbial activity. They are chemically heterogeneous, complex and difficult to define, consisting of relatively small molecules forming supramolecular associations by hydrophobic and hydrogen bonds, and sequester proteins (9, 10). Humic substances comprise of up to 70-80% of organic compounds in mineral soils and their properties strongly influence the physical properties and structure of soil (9).

The basidiomycete *Agaricus bisporus* (Lange) Imbach is the favored model for adaptation, persistence and growth in this humic-rich environment where nutrition is not readily available to primary degrading fungi (11, 12). The ability to utilize humic proteins gives the fungus an advantage over other saprobes in this complex substrate. The machinery used by *A. bisporus* to exploit the diverse mixture of nutrient resources is, however, poorly understood.

Aside from its ecological roles, *A. bisporus* is widely cultivated to produce mushrooms (**Fig. 1**) and is the basis of a multi-billion dollar industry. This cultivation involves the large-scale (megaton) biotechnological conversion of agricultural lignocellulosic wastes to high-value food with obvious extrapolations for bioenergy and biorefining. In commercial production for mushroom cultivation, the humic-rich substrate is typically derived from composted wheat

straw supplemented with gypsum and nitrogen-rich materials such as chicken and horse manures.

Our hypothesis has been that metabolic strategies and/or niche adaptations that might not be seen in the white-rot and brown-rot wood-decomposing fungi, nor in coprophilous fungi such as *C. cinerea,* may have evolved in humicolous species such as *A. bisporus*. Among the 'detritophiles', they may have a distinctly different deployment of substrate conversion enzymes or regulatory regimens in adaptation to their ecological niche, the partially degraded and humified plant litter.

Here, we report a draft 30 Mb genome and transcriptome sequence of *A. bisporus* H97, a European isolate obtained from a historically-cultivated stock of var. *bisporus*, considered to represent a member of the 'adapted' European population of the bisporic var. *bisporus* now associated with agricultural environments. We also sequenced the genome of the strain JB137-S8, belonging to the tetrasporic var. *burnettii* Kerrigan & Callac that is known only from the Sonoran desert of California, where it is associated with leaf litter in native stands of woody species. To identify *A. bisporus*-specific traits, we compared the H97 and JB137-S8 genomes with those of diverse fungi, including twelve newly sequenced species of white- and brown-rot Agaricomycotina (13). We focused annotation on gene families likely to be involved in litter decomposition and mushroom formation, and transcript profiling to reveal adaptation processes for growth on humic-rich substrates.

Results and Discussion

Genome Assembly and Gene Content. We sequenced and compared the genomes of the homokaryotic (haploid) strains H97 and JB137-S8. Sanger sequencing of the genomic DNA of strain H97 with 8.29x coverage resulted in a 30,387,844 base-pair genome assembly (**SI Appendix, Table S1**). Ninety-two genetic marker sequences selected along the 13 linkage groups (chromosomes) of *A. bisporus* (14, 15) were mapped on the H97 genome assembly to validate order and orientation of the 19 largest scaffolds (> 50kbp) (**SI Appendix, Fig. S1**). The ratio of physical lengths to genetic distances averaged 33 kbp/cM. Syntenic regions between *A. bisporus* scaffolds and chromosomes of the taxonomically related agaric *C. cinerea* were apparent after aligning *A. bisporus* scaffolds with the 36 Mb chromosome assembly from *C. cinerea* (6) (**Fig. 2A**). The 19 longest scaffolds covered all 13 *C. cinerea* chromosomes, with the largest *A. bisporus* scaffolds (1 to 6) aligning with the entire length of *C. cinerea* chromosomes. The largest syntenic blocks occur in regions with low meiotic recombination rates, no transposable elements (TEs), and tight gene spacing, where orthologous single-copy genes are overrepresented.

The second genome, of *A. bisporus* var. *burnettii* strain JB137-S8*,* was sequenced using 454

pyrosequencing and Illumina HiSeq (**SI Appendix, Table S1**). The initial assembly with 2,016 scaffolds was improved using the gapResolution program and manual scaffold joining based on synteny to *A. bisporus* var. *bisporus* H97 v2.0 (**SI Appendix, Fig. S2**) The final assembly contained 52 scaffolds > 50 kbp.

Thousands of individual repeated elements (class I and II transposons) belonging to 216 diverse families (e.g., *Gypsy*-like, *Copia*-like Long Terminal Repeats (LTRs)) cover 11.2% of the genome (**SI Appendix, Fig. 2A, Fig. S3**). Estimated insertion times suggest a series of retrotransposition bursts of *Copia*-like and *Gypsy*-like LTRs at <1 million years ago (**SI Appendix, Fig. S3**). TEs are not uniformly spread across the genome, but are mainly clustered in telomeric and centromeric regions (**Fig. 2A**). Several of the LTR elements have been observed to be actively moving from site to site within the genome (16), and this provides one possible explanation for the development of anomalies such as sectors or stroma from within otherwise healthy, stable cultures (17).

We estimated 10,438 and 11,289 protein-coding genes in the H97 and JB137-S8 genomes respectively, by combining both homology-based and *ab initio* methods (**SI Appendix, Tables S2** and **S3**), along with 1,140,000 ESTs (**SI Appendix**).

Agaricales Orthology and Evolution. Within the Agaricomycetes, the protein-coding genes of Agaricales have similar levels of divergence as in the Boletales, Russulales and Polyporales (**Fig. 2B**). Based on the sequence divergence between conserved protein sequences from *A. bisporus* and other sequenced Agaricales (e.g. *L. bicolor, S. commune, C. cinerea*), the split between the ancestors of these species has been estimated to have occurred at least 100 million years ago (**SI Appendix, Fig. S4**; 13). Nearly 83% of the predicted *A. bisporus* genes had homology with those in the public and JGI Mycocosm (18) databases, mostly to Agaricomycetes (**SI Appendix, Table S4, Fig. 2C**). To understand the *Agaricus* proteome in the context of other Agaricomycetes species, we compared the reported gene sets of six Agaricomycetes (**Fig. 2C**). *A. bisporus* shares a core set of 3,991 genes with these Agaricomycetes. Clustering of *A. bisporus* H97 proteins with those of other sequenced basidiomycete fungi revealed 5,058 clusters containing at least 10 protein members and 2 fungal taxa (**SI Appendix, Fig. S5**). The number of gene families exhibiting expansion was similar to those of related Agaricomycetes, such as *C. cinerea*, *P. ostreatus* or *S. commune*, but was lower than of *L. bicolor* (**SI Appendix, Fig. S5**).

The *A. bisporus* proteome specializations are illustrated by the over- and under-representation of protein family (PFAM) domains compared to other fungi (**SI Appendix, Tables S5-S7**). Several families of well-known detoxification enzymes were found amongst the

protein families in expansion, e.g., heme-thiolate peroxidase (HTP), methylmalonate semialdehyde dehydrogenase, beta-etherase (glutathione-S-transferases cleaving β-aryl ether linkages) and pyranose dehydrogenase, suggesting a higher ability to metabolize derivatives of lignin and other polymers abundant in humicolous habitats.

Genes Involved in Lignocellulose Decomposition. *A. bisporus* is a very poor competitor on fresh non-degraded plant wastes but competes well on partially decomposed plant litter on forest floors and grassland soils rich in humic substrates. *A. bisporus* is adapted to growing in this ecological niche, where it and other species of Agaricaceae can occur abundantly and even predominate based upon observed fructifications. To identify the genomic traits enabling *A. bisporus* to adapt to its biotope and to efficiently complete its life cycle, we have identified the repertoire and expression of genes known to be involved in organic matter degradation (carbohydrate-acting enzymes [CAZymes], lignin-related oxidoreductases, secreted proteases) and compared this arsenal to that of the 'white' and 'brown' wood-rotters, the coprophilous *C. cinerea* and the mycorrhizal symbiont *L. bicolor* (2-6, 13, 19). We also used custom microarrays to compare gene expression at four developmental stages, defined by mycelial cultures on agar-medium, mycelium colonizing the casing-soil layer or the compost (a proxy for humic-rich composted material) and mature fruiting bodies (**Fig. 1**). Amongst the most highly upregulated transcripts found in mycelium grown on compost were CAZymes, cutinases, oxidoreductases, and secreted proteases (**SI Appendix, Table S8, Fig. S6**).

Carbohydrate-acting enzymes. A. bisporus is a generalist with respect to polysaccharide degradation when grown in laboratory culture on minimal medium and specific carbon sources (**SI Appendix, Fig. S7**). It grows better (relative to glucose) on xylan than do other basidiomycetes, such as *S. commune* and *L. bicolor*. Xylan is the second most abundant polysaccharide in plant cell walls, comprising 7–12% of plant dry mass (20), and in wheat straw (21, 22). Although *A. bisporus* grows well on cellulose, it is less efficient than *S. commune* and *C. cinerea*. This catabolic ability concurs with the presence of a large set of genes encoding CAZymes (23) acting on plant, fungal and bacterial cell wall polysaccharides [including 188 glycoside hydrolases (GH), 59 polysaccharide lyases (PL) and 10 carbohydrate esterases (CE)]. Clustering of CAZyme profiles in a large set of sequenced fungi, including white- and brown-rots, plant and animal parasites, and an ectomycorrhizal symbiont showed that the CAZyme profiles deviate from species phylogeny. The total CAZyme repertoire for *A. bisporus* is similar to that of white- and brown-rot basidiomycetes (**Fig. 3**) rather than the more closely taxonomically related *C. cinerea* and *L. bicolor*. This pattern likely reflects the adaptation of *A. bisporus* to plant cell wall (PCW) polysaccharide-rich leaf litters (8). The up-regulation of

transcripts with high similarity to PCW-degrading GHs (e.g., GH5, GH6, GH7, GH12, GH61, GH105) from basidiomycetes implicated in wood decay confirms that *A. bisporus* has the generic potential to break down PCW polymers by deploying a complete suite of enzymes degrading crystalline cellulose and xylans (**Fig. 3, SI Appendix, Fig. S8, Table S10**). Notably, families GH6 and GH7 (**Fig. S8A**), which include cellobiohydrolases that are involved in the attack of crystalline cellulose (24, 25), are present in all white rot lineages and *A. bisporus*, but they are absent in brown rot lineages (except Boletales) and *L. bicolor* (**Fig. 3**).

Profiling of CAZyme transcripts from mycelium growing in compost demonstrated that 115 (51%) of GHs, PLs and CEs present in *A. bisporus* were upregulated (from 10- to 1450-fold) in compost, contrasting sharply with only 17% upregulated transcripts in both the differentiating casing-soil mycelium and the fruiting body (**SI Appendix, Fig. S6A, Table S9**). Four genes (two CE5 acetyl xylan esterases and two GH12 cellulases) showed the highest up-regulation compared to agar-grown mycelium (**SI Appendix, Table S9**). A rhamnogalacturonyl hydrolase (GH105) was induced 836-fold. Notably, growth on compost was accompanied by the up-regulation of all 16 genes encoding cellulose-binding motif (CBM1)-containing proteins. Although significantly upregulated, the pectin digestion machinery was comparatively less prominent than that for cellulose and xylan (**SI Appendix, Fig. S6A, Table S9**). The transcript profile of the mycelium growing on compost is therefore compatible with a prevailing substrate preference for xylan and cellulose, a medium activity on pectin and a slight activity on mannan. This digestion pattern is well-matched to the known composition of grasses and straw (20, 21) and sequential changes in carbohydrates during composting and mushroom growth (22).

Lignin-converting oxidoreductase genes. To gain access to cellulose, wood-decaying white-rots use fungal class II lignolytic peroxidases (PODs) to degrade lignin (13). We searched sequenced Agaricomycotina genomes for 27 gene families encoding oxidoreductases and CAZymes that have been implicated in wood decay (**SI Appendix, Fig. S9**). *A. bisporus* has a distinctive pattern that is not seen in white- and brown-rotters, *C. cinerea* and *L. bicolor*. Comparative analysis of the distribution of genes encoding lignolytic PODs [lignin peroxidase (LiP), manganese peroxidase (MnP), and versatile peroxidase (VP)] revealed that *A. bisporus* retains a limited POD machinery to degrade lignin (**SI Appendix, Table S11**). Of the genes encoding lignolytic PODs, which have been shown to be important for lignin degradation in wood decayers (13, 26, 27), only two MnP genes were found in the *A. bisporus* genome. In compost, transcript levels of one of these MnPs (MNP1, JGI ID#221245) were significantly up-regulated relative to agar medium (**SI Appendix, Fig. S6B**). Thus, the repertoire of *A. bisporus* lignolytic PODs differs from *P. chrysosporium* and other sequenced white-rot fungi, which feature 6 to 26 POD genes (**SI Appendix, Fig. S10)** (13). The number and types of lignolytic

PODs is similar to brown-rot lineages and *C. cinerea* having a single POD (13) (**SI Appendix, Table S11**). In contrast, the *A. bisporus* genome contains the largest set (24 members) of heme-thiolate peroxidase (HTP) genes, including aromatic peroxygenases (APOs) and classic chloroperoxidases (CPOs), a significant expansion relative to wood-decay fungi (**Fig. 4, SI Appendix, Table S11**) (13). Typical APOs and CPOs are secreted, versatile enzymes with multiple catalytic activities with organic hydrocarbons and lignin-like aromatic compounds, including peroxidative oxidation, epoxidation, hydroxylation and oxygen transfer reactions (27). Moreover, 16 of these HTP genes were significantly upregulated in compost relative to defined medium, including an APO induced 1492-fold (**SI Appendix, Fig. S6B, Table S12**). Several transcripts coding for beta-etherases, one of the *A. bisporus* expanding family (**SI Appendix, Table S7**), were also significantly upregulated in compost relative to agar medium (**SI Appendix, Fig. S6B**). Possibly, the number and expression patterns of *A. bisporus* HTPs and beta-etherases are related to the heterogeneous nature of humic-rich lignocellulosic materials such as compost (22, 25). To estimate patterns of duplication and loss of genes encoding HTPs in the organismal phylogeny, we performed gene tree/species tree reconciliation analyses using Notung (28). This analysis suggests that the ancestor of the Agaricomycotina possessed six HTP gene copies, and that the number of HTP paralogs has been more or less steady throughout the evolution of most Agaricomycetes (**Fig. 4**). However, an abrupt expansion of HTPs is reconstructed in the lineage leading from the common ancestor of *Agaricus, Coprinopsis* and *Laccaria*, which is reconstructed as having seven HTP gene copies, and *Agaricus*, which has 24 HTP gene copies (**Fig. 4**). Expansion of HTPs could have been an adaption for decomposition of non-woody plant matter and humic substances in soil, which is a common substrate for species of Agaricaceae.

Substrate complexity may also explain the presence of three compost-induced glyoxal oxidase-encoding genes (GLX). These copper radical oxidases are thought to play a role in production of extracellular H_2O_2 from simple aldehydes, such as glyoxal and methylglyoxal, and they are typically associated with Class II PODs (**SI Appendix, Tables S11** and **S12**). Catalytically distinct from the copper radical oxidases, at least 12 laccases *sensu stricto* were also confidently predicted (**SI Appendix, Table S11**). Three *A. bisporus* laccase-encoding genes were significantly upregulated (>10-fold, $P<0.05$) in compost relative to defined medium (**SI Appendix, Fig. 6B and Table S12**). Other potential H_2O_2-generating extracellular enzymes include various glucose-methanol-choline oxidoreductases that include a likely aryl alcohol oxidase (JGI ID#185801) and a methanol oxidase (JGI ID#195553). The gene coding for the latter enzyme is highly upregulated (**SI Appendix, Fig. 6B, Table S12**).

Intracellular metabolism of lignin metabolites and related compounds is poorly understood

but cytochrome P450s (CYPs) are generally thought to play an important role. The *A. bisporus* genome contains a relatively low number of CYPs (109 genes) (**SI Appendix, Table S11**), but many were highly expressed and regulated. Specifically, six CYP64-encoding genes were upregulated >10-fold in compost relative to defined medium (**SI Appendix, Table S12**).

Induction of protease genes on compost. Litter decomposers share the ability to utilize proteins as a sole source of carbon and nitrogen (26). The 'casing soil' layer used in cultivation is extremely nutrient poor, and induces *A. bisporus* hyphae to aggregate and form a corded morphology where nutrient transport and proteinase activity is important. In line with this view, the two sequenced *A. bisporus* genomes reflect a remarkable metabolic capability for protein degradation and remobilization through amino acid and peptide transporters. Using the MEROPS protease nomenclature, which is based on intrinsic evolutionary and structural relationships (29), we identified 111 genes coding for proteases which possessed a secretion signal (**SI Appendix, Table S13**). We did not detect in *A. bisporus* any protease unique to this species. However, several transcripts coding for serine proteases (S8, S9, S10 and S12 families) were amongst the most highly upregulated transcripts (>50-fold in comparison to agar-grown mycelium) in compost-grown mycelium (**SI Appendix, Table S14, Fig. S6C**). From the microarray data, a gene cluster coding for three serine proteases (located on chromosome 9) showed high expression on compost compared to other conditions. The most abundantly expressed of these was SPR1 (JGI ID# 194648), showing a 100-fold induction in mycelium colonizing compost which is consistent with a major role in nutrient acquisition (11). *A. bisporus* serine proteinase has been shown to be synthesized specifically in response to humic-protein complex; transgenic analysis of the SPR1 promoter elements confirmed that the promoter is able to regulate mycelial serine proteinase production in response to specific nitrogen sources (11, 30). The abundance and substrate-induction of active proteinases may enable niche specialization in *A. bisporus*.

Metabolites released during litter (and compost) decay can efficiently be taken up by *A. bisporus* mycelium colonizing this substrate, as several genes coding for monosaccharide, cellodextrins, nicotinic acid and amino acid transporters also were strikingly upregulated on compost (cluster IV in **SI Appendix, Fig. S11**).

To identify the regulatory regions involved in adaptation to humic rich environments, transcriptomic data were compared with promoter sequences. Expression ratios were calculated and ranked from the microarray data comparing *A. bisporus* growing in humic (compost) vs. non-humic (agar-medium) environments. A conserved sequence motif (TC[CA][TG]G[AT][GTA]A[AC]AATCTC) in the promoters of 23 of the top 33 compost-induced genes, occurs at a much higher rate than in orthologs of *C. cinerea* and *L. bicolor* (**SI**

Appendix, Table S15A, Fig. S12), and exists in compost-induced genes of both *A. bisporus* genomes at a frequency significantly greater than random chance (**SI Appendix, Table S15B**). It is interesting to speculate (and to ultimately determine) whether this motif, which occurs more frequently in promoters of genes very highly expressed in humic-rich substrates, forms a common regulatory mechanism governing adaptation to the ecological niche.

Mushroom development. The fruiting bodies of *A. bisporus* are the most commonly sold mushrooms in Europe and North America. However, some aspects of the sexual life cycle are poorly understood, although they are critical factors for breeding and other industrial applications. Fruiting body formation is a highly complex developmental process that has been studied in the model basidiomycetes *S. commune* and *C. cinerea* (31, 32, 33). After the substrate has been colonized and the application of specific environmental signals (reduced temperature and levels of CO_2 and 8-carbon volatiles), hyphae differentiate into the fruiting body where meiosis occurs (**Fig. 1**). The mating type loci are the master regulators of fruiting body development in fungi (31, 33). The sexually unifactorial *A. bisporus* contains only a single mating type locus (34). The locus coding for homeodomain (HD) proteins typical for the *A* mating type in bifactorial species such as *C. cinerea* and *S. commune* and for the single mating type locus in other unifactorial Agaricomycetes (35) was found on chromosome I (scaffold 1); supporting earlier studies where genes encoding specific HD proteins were cloned from several *A. bisporus* strains of distinct mating type specificities (36). On the other hand, the genes encoding conserved pheromone and pheromone receptor genes are dispersed across the genome and the unifactorial *A. bisporus* has dispensed with the *B* mating type specificity deployed by bifactorial species.

To identify genes associated with fruiting body formation, we compared transcript profiles of undifferentiated mycelium grown on agar medium, compost, or casing-soil, and of fruiting bodies (**SI Appendix, Fig. S6, Tables S8, S9, S12, S14, S16**). Of the 7,538 transcripts detected in fruiting bodies, 613 (8%) were significantly upregulated ($P < 0.05$; FDR < 0.001) in fruiting bodies in comparison to undifferentiated mycelium grown on agar medium or compost. Amongst the 50 most highly induced genes in fruiting bodies, 40% are coding for orphan, lineage-specific genes. Genes coding for hydrophobins, lectins, tyrosinases, and transcriptional factors were amongst the most highly induced genes. Hydrophobins and tyrosinases are known to accumulate in mushroom caps during *A. bisporus* fruit body development (37, 38). We compared genes induced during the fruiting body formation in *A. bisporus*, *L. bicolor* and *S. commune* to identify common developmental gene networks (**SI Appendix, Table S16A).** Only 35 and 22 homologous genes were significantly upregulated ($P < 0.05$) in both

A. bisporus/*L. bicolor* fruiting bodies or *A. bisporus*/*S. commune* fruiting bodies, respectively. Only thirteen genes were significantly upregulated ($P < 0.05$) in the fruiting bodies of these three species (*e.g.*, aromatic-ring hydroxylase, glycoside hydrolase 16, FAD linked oxidase, fatty acid desaturase), suggesting that genes induced during mushroom development are mainly clade specific.

Recently, a set of transcription factors has been identified in *S. commune* that act downstream of the mating type loci (3, 39). These transcription factor genes have orthologs in *A. bisporus* (**SI Appendix, Table S16B**). Based on transcript profiling, several of these transcription factor genes may be involved in the regulation of mushroom formation in *A. bisporus.* The DNA binding protein *pcc1* gene which leads to *A*-regulated sexual morphogenesis in *C. cinerea* (40) was highly expressed in *A. bisporus* mycelium grown on agar medium, compost, or casing, and in fruiting bodies. The expression profiles of the orthologs of *c2h2, fst3, fst4* and *hom1* were similar in *S. commune* and *A. bisporus* (*i.e.*, up-regulation of gene expression in mushrooms compared to mycelium), suggesting that these agarics share similar master developmental switches for fruiting body formation, making these genes primary targets for a functional analysis. Studying the regulatory mechanisms underlying fructification in *A. bisporus* would allow the control of mushroom pin formation, considered by mushroom growers as the most important step in managing the mushroom crop.

Our genomic and transcriptomic data suggest that *A. bisporus* has the decay machinery to decompose lignocellulosic material (i.e., xylan, hemicellulose, cellulose and lignin); yet to our knowledge, it has not been shown to decompose wood in nature. Although there are similarities in genome composition, *A. bisporus* fits neither brown rot nor white rot classifications. We hypothesized that a humicolous fungus adapted to growth in a humic-rich environment is atypical of classic wood degrading fungi, and transcriptome expression data support this view. The wide repertoire of HTP, beta-etherases, MCO, and CYP450 oxidoreductases and their striking up-regulation in mycelium colonizing compost suggest a broad mode of attack on lignin and related metabolites and an adaptation to challenges posed by complex composts. The large gene repertoire of compost-induced CAZymes and oxidoreductases, together with high protein degradation and N scavenging abilities are key features of *A. bisporus* adaptation to humic rich ecosystems.

This study reveals genetic and enzymatic mechanisms governing adaptation of *A. bisporus* to a humic rich ecological niche created by primary degradation of plant material, demonstrating the critical role such fungi contribute to soil structure and carbon sequestration.

Materials and Methods

Genome Sequencing, Assembly, and Annotation. The homokaryotic *A. bisporus* H97 and *A. bisporus* var. *burnettii* JB137-S8 strains were sequenced by whole-genome sequencing and were assembled into predicted 30.2-Mb and 32.6-Mb genomes, respectively (SI Appendix). The protein-coding genes were predicted with a combination of automated gene callers, ESTs produced from each *A. bisporus* strain, and filtering dubious genes with similarity to transposable elements (SI Appendix). In total, the gene sets included 10,438 and 11,289 predicted genes for H97 and JB137-S8, respectively; these were the basis for multigene family analyses. The *A. bisporus* H97 genome sequence can be accessed at http://jgi.doe.gov/Abisporus_var_bisporus and the *A. bisporus* var. *burnettii* JB137-S8 genome sequence can be accessed at http://genome.jgi-psf.org/Agabi_varbur_1.

Microarray Analysis of Gene Expression. Gene expression was assessed in mycelium grown on defined agar-medium, casing substrate and compost, and fruiting bodies, using specific custom 60-mer Agilent microarrays (SI Appendix).

ACKNOWLEDGEMENTS

The work conducted by the U.S. Department of Energy Joint Genome Institute is supported by the Office of Science of the U.S. Department of Energy under Contract No. DE-AC02-05CH11231. This work was also supported by the following institutions: National Institute of Agricultural Research (INRA) and the Région Lorraine Council (grants to F.M.); the Horticultural Development Company, UK provided grants for *Agaricus bisporus* custom array development and transcriptomics. We would like to thank WW Lilly, JL Lavin, JJ Mes, JA Oguiza, V Garcia-Tagua, S Bastian, L Elbourne, W Gao, E Battaglia, B Gruben, M Nadal, J van den Brink, R Finkers and AD Wiebenga for the annotation of genomic features not presented in this paper or their technical assistance.

References

1. Sánchez C (2009) Lignocellulosic residues: Biodegradation and bioconversion by fungi. *Biotechnol. Adv.* 27:185–194.
2. Martinez D, et al. (2004) Genome sequence of the lignocellulose degrading fungus *Phanerochaete chrysosporium strain* RP78. *Nat Biotechnol* 22:695-700.
3. Ohm RA, et al. (2010) Genome sequence of the model mushroom *Schizophyllum commune. Nat. Biotechnol* 28:957-963.
4. Martinez D, et al. (2009) Genome, transcriptome, and secretome analysis of wood decay fungus *Postia placenta* supports unique mechanisms of lignocellulose conversion. *Proc Natl Acad Sci USA* 106: 954-1959.
5. Eastwood DC, et al. (2011) The plant cell wall–decomposing machinery underlies the functional diversity of forest fungi. *Science* 333:762-765.
6. Stajich JE, et al. (2010) Insights into evolution of multicellular fungi from the assembled chromosomes of the mushroom *Coprinopsis cinerea (Coprinus cinereus)*. *Proc Natl Acad Sci USA* 107:11889-11894.
7. Boddy L, Watkinson SC (1995) Wood decomposition, higher fungi, and their role in nutrient redistribution. *Canadian Journal of Botany* 73:S1377-1383.
8. Sariyildiz T, Anderson JM (2005) Variation in the chemical composition of green leaves and leaf litters from three deciduous tree species growing on different soil types. *Forest Ecol Management* 210:303–319.
9. Piccolo A (2002) The supramolecular structure of humic substances. A novel understanding of humus chemistry and implications in soil science. *Adv. Agron* 75:57–134.
10. Tomaszewski JE, Schwarzenbach RP, Sander M (2011) Protein encapsulation by humic substances. *Environ Sci Technol* 45:6003–6010.
11. Burton KS, Smith JF, Wood DA, Thurston CF (1997) Extracellular proteinases from the mycelium of the cultivated mushroom (*Agaricus bisporus*). *Mycol Res* 101:1341-1347.
12. Fermor TR, Wood DA. (1981) Degradation of bacteria by *Agaricus bisporus* and other fungi. *J Gen Microbiol* 126: 377-387.
13. Floudas D, et al. (2012) The Paleozoic origin of enzymatic mechanisms for lignin decomposition reconstructed using 31 fungal genomes. *Science* 336: 1715-1719.
14. Sonnenberg AS, et al. (1996) Isolation of expressed sequence tags of *Agaricus bisporus* and their assignment to chromosomes. *Appl Environ Microbiol* 62:4542-4547.
15. Foulongne-Oriol M, et al. (2011) Comparative linkage mapping in the white button mushroom *Agaricus bisporus* provides foundation for breeding management. *Curr Genet* 57:39–50.
16. Sonnenberg ASM, Baars JJP, Mikosch TSP, Schaap PJ, Van Griensven LJLD (1999) *Abr1,* a transposon-like element in the genome of the cultivated mushroom *Agaricus bisporus* (Lange) Imbach. *Appl Environ Microbiol* 65:3347-3353.
17. Horgen PA, Carvalho D, Sonnenberg, A, Li A, Van Griensven LJLD (1996) Chromosomal abnormalities associated with strain degeneration in the cultivated mushroom, *Agaricus bisporus*. *Fungal Genet. Biol*. 20:229–241
18. Grigoriev IV, et al (2012) The genome portal of the Department of Energy Joint Genome Institute. *Nucleic Acids Res* 40:D26–D32.
19. Martin F, et al (2008) The genome of *Laccaria bicolor* provides insights into mycorrhizal symbiosis. *Nature* 452:88-92.
20. Fry SC (1988) The growing plant cell wall: chemical and metabolic analysis. The Blackburn Press, Blackburn Press, Caldwell, NJ, USA, p. 352.
21. Lawther JM, Sun R, Banks WB (1995) Extraction, fractionation, and characterization of structural polysaccharides from wheat straw. *J Agric Food Chem* 43:667-675.
22. Iiyama K, Stone BA, Macauley BJ (1994) Compositional changes in compost during composting and growth of *Agaricus bisporus*. *Appl Environ Microbiol* 60:1538-1546.
23. Cantarel BL, et al (2009) The Carbohydrate-Active EnZymes database (CAZy): an expert resource for glycogenomics. *Nucleic Acids Res* 37: D233–D238.
24. Coughlan MP, Hazlewood GP (1993) ß-1,4-D-xylan-degrading enzyme systems: biochemistry, molecular biology and applications. *Biotechnol Appl Biochem* 17:259-289.
25. Baldrian P, Valášková V (2008) Degradation of cellulose by basidiomycetous fungi. *FEMS Microbiol Rev* 32:501-521.

26. Baldrian P (2008) Enzymes of saprotrophic Basidiomycetes in *Ecology of Saprotrophic Basidiomycetes, British Mycological Society Symposia Series* 28:19-41.
27. Hofrichter M, Ullrich R, Pecyna MJ, Liers C, Lundell T (2010) New and classic families of secreted fungal heme peroxidases. *Appl Microbiol Biotech* 87: 871-897.
28. Vernot B, Stolzer M, Goldman A, Durand D (2008) Reconciliation with non-binary species trees. *J Comput Biol* 15:981-1006.
29. Rawlings ND, Barrett AJ, Bateman A (2010) MEROPS: the peptidase database. *Nucl Acid Res* 38: D227-233.
30. Heneghan MN, et al (2009) Characterisation of serine proteinase expression in *Agaricus bisporus* and *Coprinopsis cinerea* using GFP and the *A. bisporus* SPR1 promoter. *Appl Environ Microbiol* 75:792-801.
31. Kües U (2000) Life history and developmental processes in the basidiomycete *Coprinus cinereus*. *Microbiol Mol Biol Rev* 64:316–353.
32. Umar MH, Van Griensven LJLD (1997) Morphological studies on the life span, developmental stages, senescence and death of fruit bodies of *Agaricus bisporus*. *Mycol Res* 101:1409-1422.
33. Raudaskoski M, Kothe E (2010) Basidiomycete mating type genes and pheromone signaling. *Eukaryot Cell* 9:847–859
34. Xu J, Kerrigan RW, Horgen PA, Anderson J (1993) Localization of the mating type gene in *Agaricus bisporus*. *Appl Env Microbiol* 59: 3044-3049.
35. Kües U, James TY, Heitman J (2011) Mating type in Basidiomycetes: Unipolar, bipolar, and tetrapolar patterns of sexuality. *The Mycota XIV: Evolution of fungi and fungal-like organisms*, eds Pöggeler S, Wöstemeyer J (Springer, Berlin), pp 97-160.
36. Li Y, Challen M, Elliott T, Casselton L (2004) Molecular analysis of breeding behaviour in *Agaricus* species. *Mushr Sci* 16:103-109.
37. De Groot PWJ, Schaap PJ, Sonnenberg AS, Visser J, Van Griensven LJLD (1996) The *Agaricus bisporus hypA* gene encodes a hydrophobin and specifically accumulates in peel tissue of mushroom caps during fruit body development. *J Mol Biol* 257:1008-1018.
38. Soler-Rivas C, Möller AC, Arpin N, Olivier JM, Wichers HJ (2001) Induction of a tyrosinase mRNA in *Agaricus bisporus* upon treatment with a tolaasin preparation from *Pseudomonas tolaasii*. *Physiol Mol Plant Path* 58:95-99.
39. Ohm RA, de Jong JF, de Bekker C, Wösten HAB, Lugones LG (2011) Transcription factor genes of *Schizophyllum commune* involved in regulation of mushroom formation. *Mol Microbiol* 81:1433-1445
40. Murata Y, Fujii M, Zolan ME, Kamada T (1998) Molecular analysis of *pcc1*, a gene that leads to *A*-regulated sexual morphogenesis in *Coprinus cinereus*. *Genetics* 149:1753-1761.

Figure Legends

Figure 1. Developmental stages of *Agaricus bisporus* during the successive steps of its cultivation: spawning, casing, induction and 1st fruiting body flush). The vegetative (incubation, post-incubation) and fructification phases are shown. Inoculation of compost is done with wheat kernels overgrown with mycelium (spawning). In two weeks, mycelium has grown throughout the compost and induction of fruiting bodies is taking place 22 days after a change in aeration and addition of the casing layer. The first flush of fruiting bodies is observed at 32 days with a switch from mycelium extension to the production of primordia (pinning). Key physicochemical factors (relative humidity, RH%, CO_2 concentration and air temperature, T°C) are given at the bottom of the figure.

Figure 2. Agaricomycete gene orthology and evolution. (**A)** Macrosynteny between *Agaricus bisporus* var *bisporus* H97 scaffolds and *Coprinopsis cinerea* Okayama7 chromosomes. *A. bisporus* scaffolds are depicted by the colored blocks and *C. cinerea* chromosomes are represented by gray blocks. Only regions larger than 5,000 bp are connected with links of colors matching those used for coloring *A. bisporus* scaffolds. The distributions of protein coding regions and repetitive elements are shown in the outer circle, with protein coding gene density in blue and repetitive sequences in red; with a window size of 0.1 Mb. Comparison between the two genomes sequences was performed with VISTA (http://genome.lbl.gov/vista/). (**B**) The distribution of pairwise amino acid identity. Histogram shows the distribution of sequence identity of 1:1 orthologs between *A. bisporus* and *L. bicolor* (diverged ~85 million years ago)(12). To highlight the similar level of molecular divergence, 1:1 orthologs between *A. bisporus* and *C. cinerea*, 1:1 orthologs of two Boletales (*Serpula lacrymans/Coniophora puteana*), two Russulales (*Heterobasidion annosum/Stereum hirsutum*) and two Polyporales (*Trametes versicolor/Dichomitus squalens*) were plotted in red, blue, green and black, respectively. (**C**) Orthology assignment of seven Agaricomycete genomes. Bars are subdivided to represent different types of orthology relationships. 1:1:1 indicates universal single-copy genes; N:N:N indicates other universal genes, but absence in a single genome within the different orders is tolerated. Order specific indicates Polyporales, Russulales, Boletales or Agaricales specific genes ; Fungi indicated fungi-specific orthologs; Duplicated species specific indicates species-specific duplicated genes; Species specific indicated species-specific genes (orphans).

Figure 3. Double clustering of the carbohydrate-cleaving enzyme families (CAZymes) from representative fungal genomes. Top tree: fungal species. Left tree: the enzyme families are represented by their class (GH, glycoside hydrolase; PL, polysaccharide lyase) and family number according to the carbohydrate-active enzyme database (19). Right side: known substrate of CAZy families (most common forms in brackets): BPG, bacterial peptidoglycan; BEPS, bacterial exopolysaccharides; CW, cell wall; ESR, energy storage and recovery; FCW, fungal cell wall; PCW, plant cell wall; PG, protein glycosylation; U, undetermined; α-gluc, α-glucans (including starch/glycogen); β-glyc, β-glycans; β-1,3-gluc, β-1,3-glucan; cell, cellulose; chit, chitin/chitosan; dext, dextran; hemi, hemicelluloses; inul, inulin; N-glyc, N-glycans; N-/O-glyc, N- / O-glycans; pect, pectin; sucr, sucrose; and tre, trehalose. Abundance of the different enzymes within a family is represented by a color scale from 0 (black) to 44 occurrences (red) per species. In the top tree, black circles, plant and fungal pathogens; red squares, humicolous saprotrophs; white squares, white rots; orange circles, brown-rots; green triangle, ectomycorrhizal symbiont.

Figure 4. The expansion of HTP-s in *Agaricus bisporus*. (A) HTP copy numbers at internal nodes in the Agaricomycetes as reconstructed by gene-tree species-tree reconciliations in Notung (28) under two edge weight threshold values. Numbers after species names denote the extant copy numbers of HTP-s found in the genomes of these species. (B) Maximum Clade credibility chronogram of heme-thiolate peroxidases of the Agaricomycetes showing six independent lineages of HTPs in *Agaricus bisporus*. Branch lengths correspond to relative time. Thickened branches are strongly supported by Maximum Likelihood bootstrap and Bayesian posterior probabilities.



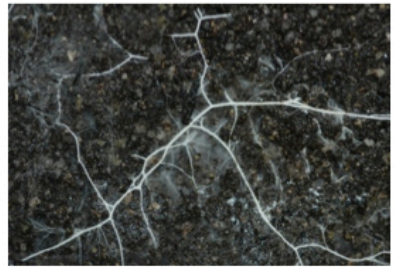
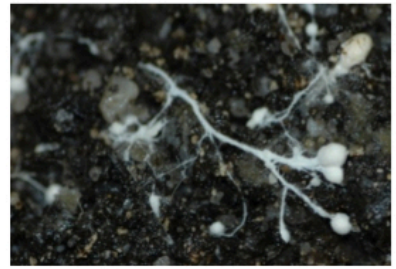


Vegetative phase																					Fruiting phase											
Incubation												Post-incubation									Fructification											
1	2	3	4	5	6	7	8	9	10	11	12	13	14	15	16	17	18	19	20	21	22	23	24	25	26	27	28	29	30	31	32
days																															

Spawning

Spawn running

Casing

Case running
Initiation stage with aggregation of mycelium into hyphal cords

Induction

Primordia formation
Development of first fruiting bodies

1st Flush

RH ≤ 100%

≅ 85 – 95 %

CO_2 ≤ 2%

≅ 0.1 – 0.13 %

Air Temperature ≅ 25°C

≅ 17 °C

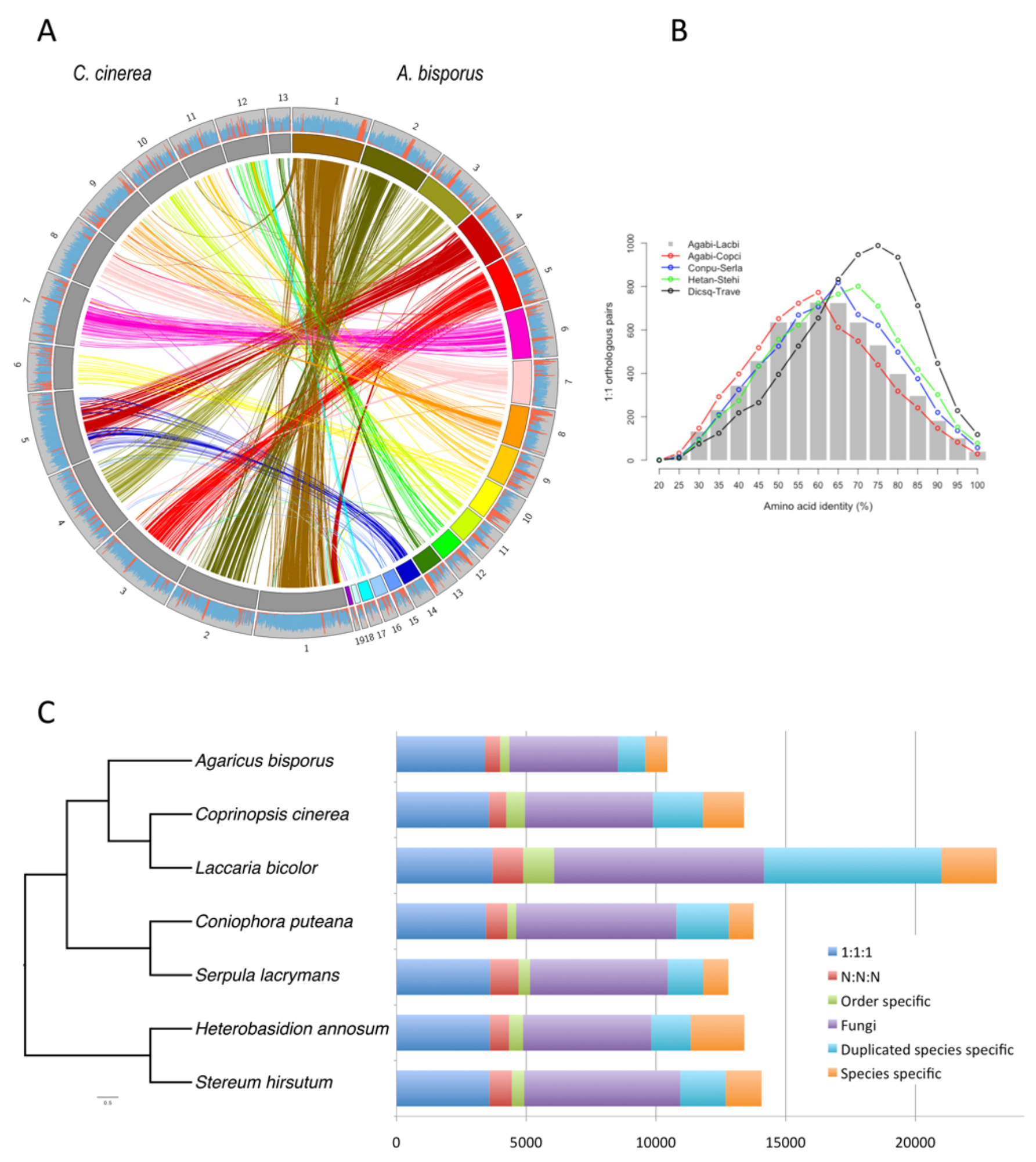
A
C. cinerea
A. bisporus
B
Agabi-Lacbi
Agabi-Copci
Conpu-Serla
Hetan-Stehi
Dicsq-Trave
1:1 orthologous pairs
Amino acid identity (%)
C
Agaricus bisporus
Coprinopsis cinerea
Laccaria bicolor
Coniophora puteana
Serpula lacrymans
Heterobasidion annosum
Stereum hirsutum
1:1:1
N:N:N
Order specific
Fungi
Duplicated species specific
Species specific

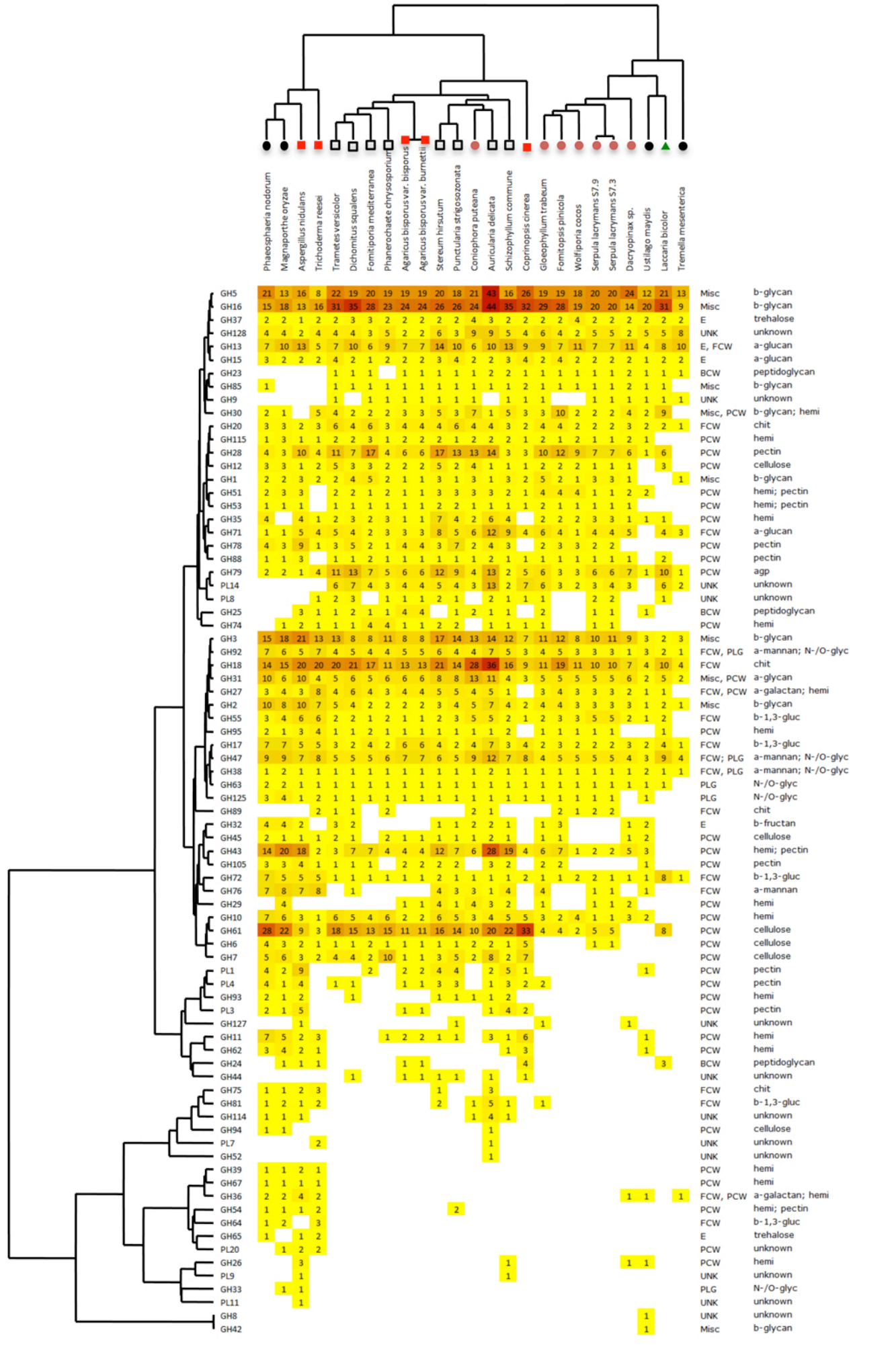
Phaeosphaeria nodorum
Magnaporthe oryzae
Aspergillus nidulans
Trichoderma reesei
Trametes versicolor
Dichomitus squalens
Fomitiporia mediterranea
Phanerochaete chrysosporium
Agaricus bisporus var. bisporus
Agaricus bisporus var. burnettii
Stereum hirsutum
Punctularia strigosozonata
Coniophora puteana
Auricularia delicata
Schizophyllum commune
Coprinopsis cinerea
Gloeophyllum trabeum
Fomitopsis pinicola
Wolfiporia cocos
Serpula lacrymans S7.9
Serpula lacrymans S7.3
Dacryopinax sp.
Ustilago maydis
Laccaria bicolor
Tremella mesenterica
GH5 Misc b-glycan
GH16 Misc b-glycan
GH37 E trehalose
GH128 UNK unknown
GH13 E, FCW a-glucan
GH15 E a-glucan
GH23 BCW peptidoglycan
GH85 Misc b-glycan
GH9 UNK unknown
GH30 Misc, PCW b-glycan; hemi
GH20 FCW chit
GH115 PCW hemi
GH28 PCW pectin
GH12 PCW cellulose
GH1 Misc b-glycan
GH51 PCW hemi; pectin
GH53 PCW hemi; pectin
GH35 PCW hemi
GH71 FCW a-glucan
GH78 PCW pectin
GH88 PCW pectin
GH79 PCW agp
PL14 UNK unknown
PL8 UNK unknown
GH25 BCW peptidoglycan
GH74 PCW hemi
GH3 Misc b-glycan
GH92 FCW, PLG a-mannan; N-/O-glyc
GH18 FCW chit
GH31 Misc, PCW a-glycan
GH27 FCW, PCW a-galactan; hemi
GH2 Misc b-glycan
GH55 FCW b-1,3-gluc
GH95 PCW hemi
GH17 FCW b-1,3-gluc
GH47 FCW; PLG a-mannan; N-/O-glyc
GH38 FCW, PLG a-mannan; N-/O-glyc
GH63 PLG N-/O-glyc
GH125 PLG N-/O-glyc
GH89 FCW chit
GH32 E b-fructan
GH45 PCW cellulose
GH43 PCW hemi; pectin
GH105 PCW pectin
GH72 FCW b-1,3-gluc
GH76 FCW a-mannan
GH29 PCW hemi
GH10 PCW hemi
GH61 PCW cellulose
GH6 PCW cellulose
GH7 PCW cellulose
PL1 PCW pectin
PL4 PCW pectin
GH93 PCW hemi
PL3 PCW pectin
GH127 UNK unknown
GH11 PCW hemi
GH62 PCW hemi
GH24 BCW peptidoglycan
GH44 UNK unknown
GH75 FCW chit
GH81 FCW b-1,3-gluc
GH114 UNK unknown
GH94 PCW cellulose
PL7 UNK unknown
GH52 UNK unknown
GH39 PCW hemi
GH67 PCW hemi
GH36 FCW, PCW a-galactan; hemi
GH54 PCW hemi; pectin
GH64 FCW b-1,3-gluc
GH65 E trehalose
PL20 PCW unknown
GH26 PCW hemi
PL9 UNK unknown
GH33 PLG N-/O-glyc
PL11 UNK unknown
GH8 UNK unknown
GH42 Misc b-glycan

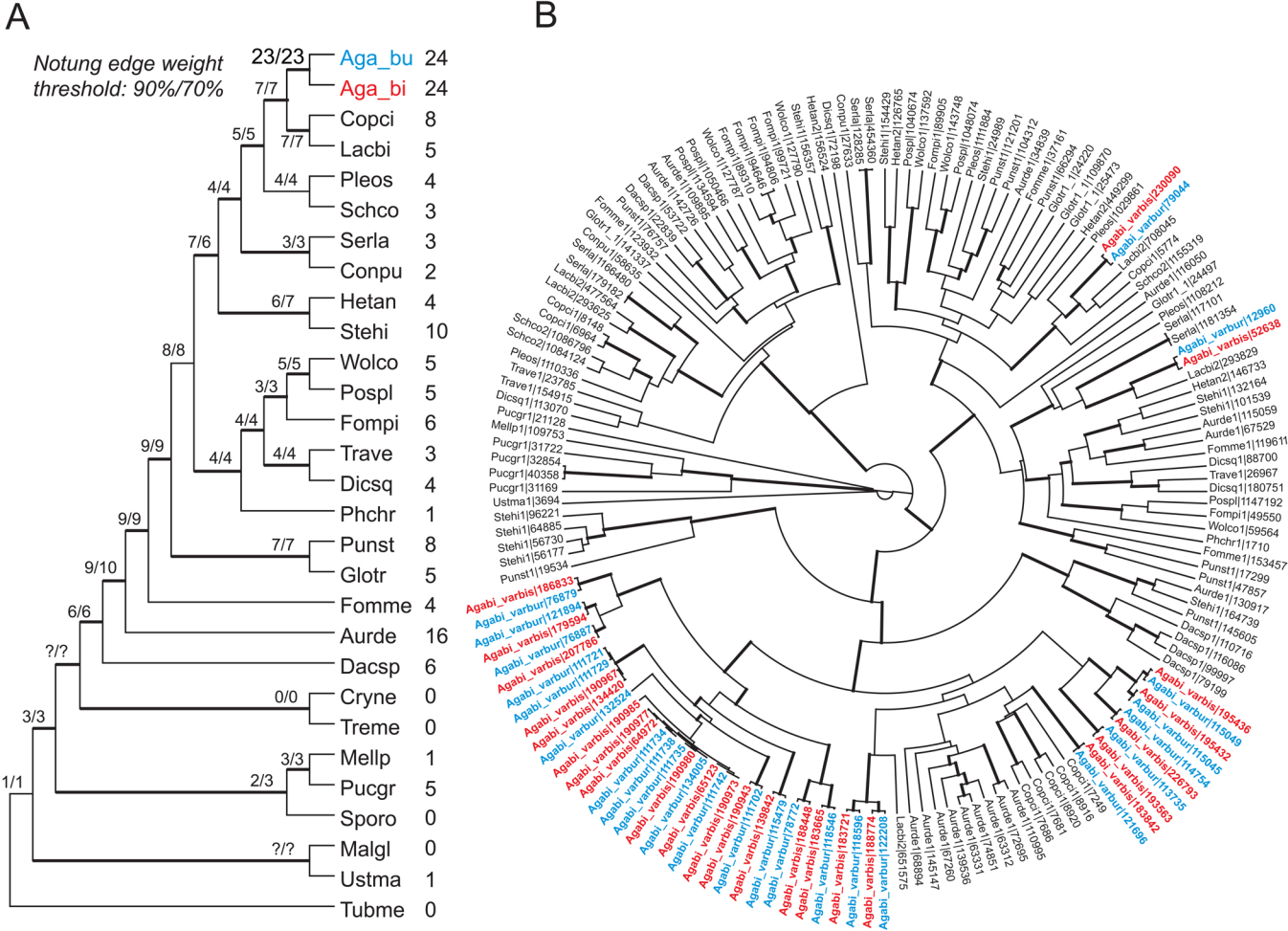
A
Notung edge weight threshold: 90%/70%
23/23
7/7
5/5
7/7
4/4
4/4
7/6
3/3
6/7
8/8
5/5
3/3
4/4
9/9
4/4
4/4
9/9
7/7
9/10
6/6
?/?
0/0
3/3
3/3
1/1
2/3
?/?
Aga_bu 24
Aga_bi 24
Copci 8
Lacbi 5
Pleos 4
Schco 3
Serla 3
Conpu 2
Hetan 4
Stehi 10
Wolco 5
Pospl 5
Fompi 6
Trave 3
Dicsq 4
Phchr 1
Punst 8
Glotr 5
Fomme 4
Aurde 16
Dacsp 6
Cryne 0
Treme 0
Mellp 1
Pucgr 5
Sporo 0
Malgl 0
Ustma 1
Tubme 0
B